Green Chemistry

Cite this: *Green Chem.*, 2012, **14**, 2856

www.rsc.org/greenchem

PAPER

Kinetics and pathways for an algal phospholipid (1,2-dioleoyl-*sn*-glycero-3-phosphocholine) in high-temperature (175–350 °C) water

Shujauddin Changi,[a] Adam J. Matzger[b] and Phillip E. Savage*[a]

Received 26th April 2012, Accepted 10th July 2012
DOI: 10.1039/c2gc35639b

We examined the behavior of 1,2-dioleoyl-*sn*-glycero-3-phosphocholine (DOPC) in high-temperature water at 175, 200, 225, and 350 °C. DOPC hydrolyzed to give oleic acid and a number of phosphorus-containing products. The hydrolysis was catalyzed by oleic and phosphoric acids, which were also reaction products. DOPC formed 1-acyl and 2-acyl lyso-phosphatidylcholine (LPC) along with oleic acid as primary products. LPC subsequently formed other phosphorus-containing intermediates, which finally led to phosphoric acid as the ultimate P-containing product. At 350 °C, phosphoric acid and oleic acid were the only products observed. We observed an ester of oleic acid and glycerol (9-octadecenoic-2,3-dihydroxypropyl ester), which likely formed *via* the hydrolysis of LPC. A reaction network is proposed to explain the formation of the observed products. A quantitative kinetics model based on the proposed pathways was consistent with the experimental data.

1 Introduction

Research on fuels from biomass is actively being conducted to help meet the increasing energy demand of the world's population. Of the different types of biomass sources, algae are promising because of their high photosynthetic efficiency (~20 times that of terrestrial plants),[1] their ability to grow in brackish and sea water, and their lipid content per area of land cultivated exceeding that of oil seed crops such as soy, sunflower, or palm.[2] Of course, there are also challenges associated with algae cultivation for biofuel production, and these include water supply and management and sustainable use of nutrients.

Hydrothermal processing of algal biomass has been widely reported in the past. It can be used to convert wet algal biomass to crude bio-oils,[3] carbonized solids,[4,5] and fuel gases.[6] Hydrothermal carbonization (HTC) provides a route to algal biodiesel that avoids algae drying and the use of organic solvents for lipid extraction. Hydrothermal liquefaction (HTL) of microalgae is a potentially promising route to obtain high-energy-density, fungible advanced biofuels. Both processes treat algal biomass in an aqueous medium at elevated temperatures (175–350 °C) and pressures (0.9–17 MPa). Water has distinctly different properties at high temperatures and pressures than at ambient conditions. For example, water at high temperature and high pressure has a lower dielectric constant, higher dissociation constant, and increased solubility of organic compounds.[7] Thus, biomacromolecules in algae are more susceptible to hydrolytic attack under these conditions. Hydrothermal processing is well suited for wet biomass because it obviates the need to dry the feedstock, an energy-intensive pretreatment step that lowers the overall efficiency of the process. Of course, energy inputs are also required for hydrothermal processing, but the thermal energy can be more easily recovered *via* heat integration because it will be available at a higher temperature. Moreover, hydrothermal processing has the added advantage of requiring a thermal energy input that is lower than the heat of vaporization of water, as required in drying.

Algae biomass is a complex mixture of biomacromolecules such as polysaccharides, lipids, proteins, and chlorophyll. The study of model compounds containing the same functional groups as the corresponding biomacromolecules can provide useful insight and understanding into the reaction products, pathways, kinetics, and mechanisms of hydrothermal treatment of actual biomass. We recently reported on the hydrothermal reactions of ethyl oleate,[8,9] phytol,[10] and phenylalanine[11] as model compounds representing ester linkages in triglycerides, a chlorophyll moiety, and amino acids, respectively. In this article, we use 1,2-dioleoyl-*sn*-glycero-3-phosphocholine (DOPC) as a model compound to elucidate the reactions of algal phospholipids during hydrothermal carbonization and liquefaction.

Phospholipids are an important class of lipids and can constitute 10–50 wt% of the total lipids in algae.[12] They contain a glycerol backbone with a diglyceride, a phosphate group, and an organic group. Since phospholipids contain a hydrophobic portion comprised of non-polar *n*-alkyl chains and a hydrophilic portion that contains heteroatoms such as phosphorus and nitrogen, the products obtained from their reaction in high-temperature water (HTW) can partition not only into the organic phase (*e.g.*, hydrochar, crude bio-oil) but also the aqueous phase during HTC or HTL of algae. A step following HTC or HTL of

[a]*Chemical Engineering Department, University of Michigan, Ann Arbor, MI 48109, USA. E-mail: psavage@umich.edu; Fax: +734-763-0459; Tel: +734-764-3386*
[b]*Chemistry Department, University of Michigan, Ann Arbor, MI 48109, USA*

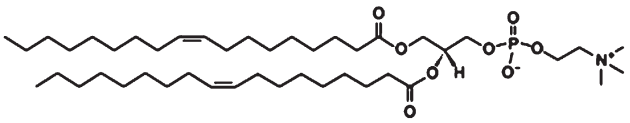

Fig. 1 Structure of DOPC.

algae is recycling the aqueous phase to grow more biomass. Ideally, all of the phosphorus in the biomass would partition into the aqueous phase after reaction to facilitate it's recycling and reuse as a nutrient. Clearly, understanding the kinetics and pathways for formation of the different P-containing compounds from phospholipids would inform the design and optimization of HTC and HTL processes. With this motivation, we studied the reactions of a phospholipid in HTW.

Bailey and Northcote found that phosphatidylcholine (PC) was the major phospholipid present in the green alga *Hydrodictyon africanum* (around 40% of the cell weight).[13] Moreover, oleic acid is known to be an abundant fatty acid in green algae.[3,14] We chose DOPC as a model phospholipid because it contains oleate moieties and a choline group, each attached to the glycerol backbone (see Fig. 1).

To the best of our knowledge, phospholipid behavior in HTW has not been reported previously. However, research has been conducted at much lower temperatures for phospholipids in liposomes and bilayers. Zuidam and Crommelin studied the kinetics of hydrolysis of phospholipid in liposomes comprising egg phosphatidylcholine (EPC), dimyristoyl phosphatidylcholine, distearoyl phosphatidylcholine, and dipalmitoyl phosphatidylcholine/cholesterol (DPPC/CHOL) at a pH of 4.0 and different temperatures (maximum 80 °C).[15] They modeled the disappearance of the phospholipid with pseudo-first-order kinetics. They have also shown that changes in fatty acid chains and size do not influence the hydrolysis rate constants significantly.

Kensil and Dennis studied the alkaline hydrolysis (pH 12.7) of EPC and DPPC in liposomes and in mixed micelles between 15–60 °C.[16] Free fatty acids and *sn*-glycerol-3-phosphorylcholine (GPC) were the main products. These authors proposed that GPC was formed though a lyso-phosphatidylcholine (LPC) intermediate. The first step of their proposed scheme involves the attack of a hydroxide ion at either the *syn*-1 or *syn*-2 positions of the PC to produce 2-acyl LPC and 1-acyl LPC isomers, respectively. The authors found equal hydrolysis rates at both positions over the first half-life of the hydrolysis process. The next step of the reaction scheme involves the hydrolysis of either of the LPCs (1-acyl and 2-acyl) to remove a second fatty acid moiety and to form GPC. The authors reported the kinetics to be first order for both the phosphatidylcholine and the hydroxide ions. They did not observe further hydrolysis of GPC and mentioned that this reaction was slow under their conditions. Hanahan have also mentioned in their review that further hydrolysis of GPC is quite slow compared to acyl hydrolysis.[17]

Grit and coworkers studied the hydrolysis of different phosphatidylcholines (PC) in aqueous liposomal dispersions under acidic and alkaline conditions and reported pseudo-first order kinetics.[18–20] They demonstrated that the rate of hydrolysis was acid- and base-catalyzed with a minimum rate occurring at a pH of 6.5 between 40–70 °C. They proposed a reaction scheme similar to Kensil and Dennis,[16] except that they observed further hydrolysis of GPC to form glycerophosphoric acid (GPA) as the end product. GPA did not hydrolyze further under their conditions. The initial hydrolysis of PC gave an isomeric mixture of 1-acyl LPC and 2-acyl LPC. However, no rate constants were reported for the individual reaction steps of their network.

Koning and McMullan studied the hydrolysis of DOPC using a 2 N HCl solution at 120 °C.[21] They too proposed a reaction network similar to Kensil and Dennis,[16] according to which the first steps involve removal of two fatty acids from the PC to form GPC. Additionally, they also suggest that GPC is further hydrolyzed *via* a cyclic *ortho* triester to form choline and cyclic glycerophosphate. Cyclic glycerophosphate was eventually converted to an equilibrium mixture of 85% α-glycerophosphate and 15% of β-glycerophosphate in the acidic medium. The authors obtained 80 ± 5% of the initial phosphorus in the combined α- and β-glycerophosphates. Maruo and Benson have shown that the rate of hydrolysis of cyclic glycerophosphate to α- and β-glycerophosphate is rapid in 0.1 N HCl and 24 °C, with 50% conversion being achieved in less than 10 min under these conditions.[22] Koning and McMullan also quantified small amounts of phosphorylcholine (15 ± 5% of total phosphorus).[21] They proposed that phosphorylcholine could form *via* the hydrolysis of the phosphate group in GPC, a reaction parallel to the formation of cyclic glycerophosphate from GPC. Lastly 5 ± 3% of inorganic phosphorus compound was quantified and hypothesized to originate *via* the hydrolysis of glycerophosphate and phosphorylcholine. However, no kinetics was reported for the individual steps of the reaction network.

It should be emphasized that although the above studies are done using liposomes and at low temperatures, they give useful information about the products that are formed during the hydrolysis of phosphatidylcholine. However, the reaction chemistry and mechanism of phosphatidylcholine is not well understood at higher temperatures (greater than 120 °C). A complete carbon or phosphorus balance remains elusive in the literature. Moreover, all of the above studies report an overall first-order rate constant for disappearance of PC. No one has yet explored the reaction at higher concentrations of PC, wherein some other kinetic phenomenon (*e.g.*, autocatalysis) may become prominent.[8] Although, researchers have proposed different reaction networks for hydrolysis of phospholipids, none of the reports mention the rate constants for all of the individual steps of the network. This article fills these gaps in the literature by reporting on DOPC reactions from 175–350 °C in HTW and providing a detailed product distribution and kinetics for the complete DOPC hydrothermal reaction network. These results have implications for understanding the behavior of phospholipids during the HTC and HTL of algae.

2 Materials and experimental methods

All experiments were carried out in batch reactors assembled from 3/8 – inch 316 stainless steel Swagelok tube fittings (one port connector and two caps). Each reactor had an internal volume of approximately 1.5 mL. Prior to initial use of these reactors, they were conditioned by filling them with water and heating in a fluidized sand bath at 300 °C for 60 min to remove any residual materials and expose the reactor walls to the HTW environment.

DOPC and LPC were purchased in high purity (>99%) from Avanti Polar Lipids Inc. Ethyl oleate, oleic acid, and a high purity TraceCERT® phosphorus standard of 1000 ± 4 mg L^{-1} phosphorus in water was purchased from Sigma Aldrich. Methanol and acetic acid (HPLC grade) were purchased from Fisher Scientific in high purity (≥99%) and used as received. Water was distilled prior to use.

Reactors (capacity 1.5 mL) were loaded at room temperature with approximately 75 mg of DOPC. The exact weight of DOPC added to the reactor was calculated as the difference in the weight of the reactor before and after loading. The amount of water loaded in the reactors was such that the aqueous fluid phase occupied 95% of the reactor volume at the reaction conditions, based on the density of pure water at the same conditions (*i.e.*, 1.27, 1.23, 1.18, and 0.92 mL of water was loaded at 175, 200, 225, and 350 °C). The pressure at reaction conditions can be estimated from the saturated steam tables as 0.9, 1.6, 2.5, and 17.0 MPa at 175, 200, 225, and 350 °C, respectively. All concentrations were based on the fluid phase volume being 95% of the reactor volume. The initial concentration of DOPC ($C_{DOPC,\ ini}$) in all experiments was about 0.07 mol L^{-1}. The loaded reactors were sealed and placed in a preheated, fluidized sand bath (Techne SBL-2D) and maintained at the desired temperature using a temperature controller (Techne TC-8D). The sand bath was isothermal within ±1 °C. The reactor heat-up time has been measured previously to be 2–3 min,[8] which is short relative to the typical batch holding times used in this study. Upon reaching the desired batch holding time, the reactors were removed from the sand bath and quenched by immersing them in a cold-water bath. The reactors were opened and the contents were recovered using methanol.

A control experiment at room temperature was used to determine the recovery of DOPC. A reactor was loaded with 20 mg of DOPC and 1.23 mL of water. The sealed reactor was kept at room temperature for 30 min. The post-reaction work-up procedure used for the experiments at the elevated temperatures was then performed. This experiment gave an average DOPC recovery of 98%, thereby verifying the suitability of the methods used for quantifying the amount of DOPC.

We analyzed oleic acid (hydrolysis product of DOPC) with HPLC and a UV detector using the method outlined previously.[8] We used an Agilent Technologies model 6890N GC equipped with an autosampler, autoinjector, and mass spectrometric detector to identify some of the products from the HTW treatment of DOPC. A Wiley mass spectral library was used for compound identification by matching the mass spectra of observed chromatogram peaks with those in the library. An Agilent Technologies model 6890 GC equipped with a FID was used to quantify the products. The reaction products were separated on a HP-5MS fused silica, non-polar capillary column (50 m length × 0.20 mm inner diameter × 0.33 μm film thickness). We used an inlet temperature of 300 °C, a split ratio of 5 : 1, and an injection volume of 1.0 μL. The temperature program involved an initial oven temperature of 50 °C followed by heating to 300 °C at a rate of 25 °C min^{-1} (isothermal for 10 min), giving a total run time of 20 min. Helium served as the carrier gas (1 mL min^{-1}). As will be discussed in the next section, the major products that we identified using the GC were glycerol and 9-octadecenoic-2,3-dihydroxypropyl ester, an ester of oleic acid and glycerol (referred to as OPE here onwards). Since, a pure standard of OPE was not available, we generated a calibration curve with different amounts of another similar ester (ethyl oleate) to quantify OPE. The glycerol peak was not well resolved, especially at high temperatures and long batch holding times, and therefore not quantified. To determine whether diglycerides were among the reaction products, we used a high temperature ASTM 6584 column installed in an Agilent GC-FID 7890 equipment and the procedure outlined previously by Levine *et al.*[4]

We identified and quantified a number of the phosphorus-containing compounds generated during the reaction of DOPC by using ^{31}P-NMR at 25 °C on a Varian MR-400 NMR spectrometer at 161.7 MHz. The inverse gated decoupling technique was used to suppress the Nuclear Overhauser Effect (NOE). An observation frequency of 1619.2 Hz was used for acquisition. A pulse angle of 90° and a relaxation delay of 10 s were utilized. Typically, we obtained 128 scans before Fourier transformation was carried out. Agilent's VnmrJ 3 software *qEstimate* tool enabled us to estimate the absolute concentration (in terms of phosphorus equivalent) for any sample. This capability is based on the linearity of the digital receiver and does not require the use of reference signals or the addition of reference standard compounds to the NMR sample. A one-point external calibration was performed for the probe before using the quantification tool. This calibration was set up using a phosphorus standard of 1000 mg L^{-1} or 32.26 mM equivalent of phosphorus (obtained from Sigma Aldrich) and the methodology outlined for calibrating the probe.[23] We tested the validity of this calibration by running phosphorus standards of known concentrations, which gave concentrations within ±5% of the actual concentration. Having established confidence in the external calibration, we quantified DOPC and other phosphorus-containing compounds using this technique. Next, we identified the products corresponding to different peaks in the NMR spectrum by matching their chemical shifts with those of pure compounds that were expected as products from the hydrolysis of DOPC. To confirm these identities, we added small amounts of these pure compounds to a sample obtained from reaction at 175 °C and 150 min. No new peaks appeared in the NMR spectrum. Rather, the areas of existing peaks increased, thereby confirming the product identities.

Product molar yields were calculated by dividing the number of moles of the product formed by the number of moles of DOPC initially loaded into the reactor. Experiments at 175 °C and 30 min, 200 °C and 45 min, and 225 °C and 45 min were carried out in triplicate to assess reproducibility.

3 Results and discussion

In this section we report the product distribution, elucidate the reaction pathways, and develop a corresponding quantitative -phenomenological kinetics model that is consistent with the experimental data.

3.1 Reaction products

Fig. 2 shows the NMR spectrum of a sample from reaction of DOPC at 200 °C and 60 min along with the identities of several products. We have positive identification for peaks 1–4, but we

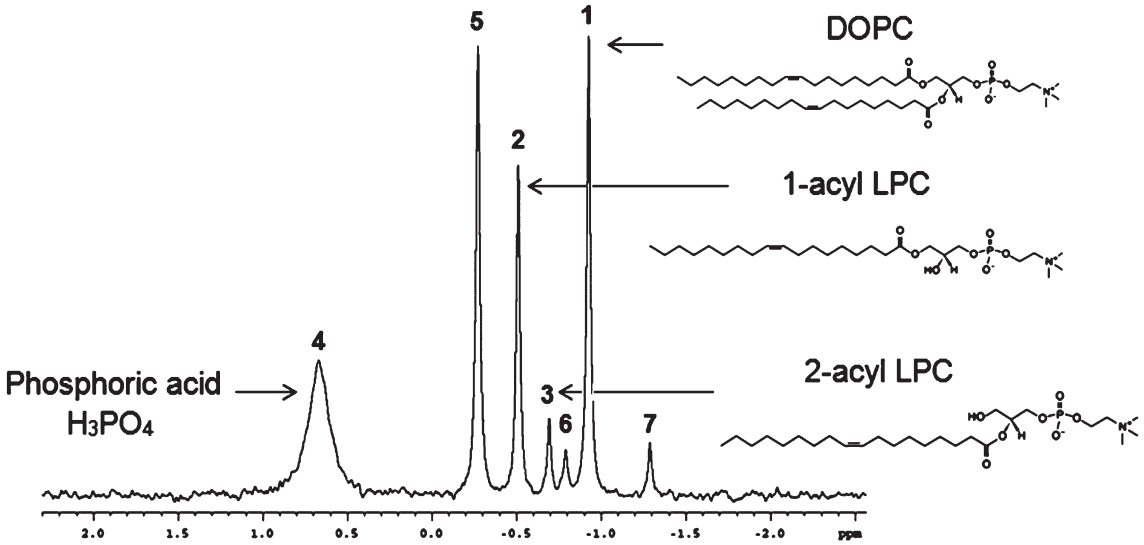

Fig. 2 ^{31}P NMR spectrum of products from DOPC reaction at 200 °C and 60 min.

were not able to identify with certainty the compounds corresponding to peaks 5–7 due to lack of authentic compounds as standards. As will be discussed later in this section, using the yields of these products and knowledge of likely pathways from the literature, we tentatively identified peaks 5, 6, and 7.

Table 1 presents the product molar yields and DOPC conversion at different times and temperatures. The mean carbon balance was 90 ± 15%. We expect the carbon balance to be below 100% since we have not quantified some of the carbon-containing products, such as glycerol and choline. The mean phosphorus balance was 95 ± 15%, indicating that all of the phosphorus-containing compounds were identified and quantified.

1-Acyl LPC was the major phosphorus-containing product at short batch holding times. Smaller amounts of 2-acyl LPC also formed. The yields of 1-acyl LPC at the two lower temperatures initially increased with increasing batch holding time, reached a maximum value, and then decreased. This behavior suggests that 1-acyl LPC decomposes to secondary products under the more severe reaction conditions. The yields of 2-acyl LPC were low (<0.05) at all conditions, but they followed a trend similar to that of 1-acyl LPC. That is, the yield of 2-acyl LPC initially increased and then subsequently decreased at longer batch holding times and higher temperatures.

Phosphoric acid was not observed at the mildest reaction conditions, but once formed, its yield rapidly increased. It became the major phosphorus-containing product at higher temperature or longer batch holding time. Yields of essentially unity were obtained at the most severe conditions, indicating that phosphoric acid is the ultimate phosphorus-containing product from the hydrolysis of DOPC.

Oleic acid, the fatty acid obtained *via* the hydrolysis of DOPC, was always the product formed in highest yield. The yield of oleic acid increased steadily with time at all temperatures. The molar yields of oleic acid may exceed unity because one mole of DOPC can produce two moles of oleic acid. At 350 °C, this stoichiometric yield of oleic acid of two was obtained, indicating that this fatty acid was another end product of the hydrolysis of DOPC.

An ester of oleic acid and glycerol was another non-phosphorus-containing product that was quantified. The yield of the 9-octadecenoic-2,3-dihydroxypropyl ester (OPE) increased steadily with time at 175 and 200 °C. At 225 °C, however, the yield of OPE first increased from 0.04 at 15 min to 0.13 at 45 min and then decreased to 0.03 at 90 min, indicating secondary decomposition of OPE. No OPE was detected at 350 °C.

Of the three tentatively identified NMR peaks (peak 5, 6, and 7 in Fig. 2), the molar yield of peak 5 is the highest at all conditions. The yields of the products corresponding to peaks 5 and 6 responded to time and temperature very much like the yield of OPE. These yields increased with an increase in the batch holding time at 175 and 200 °C, but at 225 °C they reached a maximum and then decreased to zero. Furthermore, the yield of peak 5 at the shortest time at any temperature is similar to the yield of OPE formed under similar conditions. This observation of peak 5 being formed nearly in a molar equivalence to OPE and the formation of OPE requiring the co-formation of a P-containing co-product, suggests that peak 5 could possibly be this co-product. We speculate that peak 5 corresponds to phosphorylcholine, which is the P-containing compound that would be formed along with OPE, as will be described in the next section. Phosphorylcholine has been observed previously during the acidic hydrolysis of DOPC.[21] The yield of peak 5 does not remain equal to that of OPE at higher temperatures or longer batch holding times. Rather, its yield exceeds that of OPE at the more severe conditions, even before the yield of OPE begins to decrease. This behavior indicates that if peak 5 is indeed phosphorylcholine, then as the batch holding time increases at 175 and 200 °C, there is also another pathway forming phosphorylcholine. As will be shown in the next section, phosphorylcholine can indeed be formed through a parallel reaction involving hydrolysis of the LPC isomers. Furthermore, at a higher temperature of 225 °C, the yield of peak 5 is lower than OPE

Table 1 Conversion and molar yields of products from DOPC reaction in HTW. Yields corresponding to peaks 5, 6, and 7 are based on tentative structures

Temp (°C)	Time (min)	$C_{DOPC, ipi}$ (mol L^{-1})	DOPC Conversion	1-Acyl LPC Yield	2-Acyl LPC yield	H_3PO_4 yield	Peak 5 yield	Peak 6 yield	Peak 7 yield	OA yield	OPE yield	C-balance (%)	P-balance (%)
175	30	0.071 ± 0.002	0.05 ± 0.04	0.08 ± 0.04	0.02 ± 0.007	0	0.01 ± 0.01	0	0	0.11 ± 0.05	0.01 ± 0.005	106 ± 4	106 ± 4
	60	0.067	0.14	0.16	0.03	0	0.03	0	0	0.3	0.04	112	109
	90	0.067	0.36	0.25	0.04	0	0.08	0	0.016	0.58	0.06	109	103
	120	0.068	0.67	0.22	0.03	0.03	0.18	0.006	0.024	0.76	0.07	85	81
	150	0.067	0.85	0.13	0.02	0.13	0.30	0.023	0.014	1.08	0.12	78	78
200	15	0.068	0.10	0.08	0.02	0	0	0	0	0.13	0.02	102	100
	30	0.069	0.31	0.20	0.05	0	0.05	0	0.009	0.41	0.03	103	100
	45	0.067 ± 0.001	0.67 ± 0.03	0.18 ± 0.02	0.04 ± 0.004	0.13 ± 0.01	0.13 ± 0.002	0.014 ± 0.004	0.02 ± 0.001	0.56 ± 0.08	0.04 ± 0.004	73 ± 7	84 ± 4
	60	0.067	0.82	0.13	0.03	0.27	0.19		0.021	0.82	0.08	68	88
	90	0.067	0.94	0.04	0.01	0.60	0.23	0.021	0.006	1.39	0.11	74	101
225	15	0.068	0.36	0.19	0.04	0.15	0.06	0	0.019	0.48	0.04	99	109
	30	0.069	0.85	0.05	0.01	0.74	0.11	0.008	0.008	1.18	0.16	75	112
	45	0.067 ± 0.001	0.97 ± 0.01	0.01 ± 0.003	0	0.94 ± 0.02	0.08 ± 0.00	0	0	1.39 ± 0.03	0.13 ± 0.02	67 ± 2	110 ± 2
	60	0.067	1	0	0	1.05	0.04	0	0	1.7	0.09	75	112
	90	0.069	1	0	0	1.18	0	0	0	1.91	0.03	80	110
350	15	0.069	1	0	0	0.94	0	0	0	2.00	0	82	94
	30	0.068	1	0	0	0.90	0	0	0	1.91	0	78	90
	45	0.068	1	0	0	0.92	0	0	0	2.00	0	82	92
	60	0.070	1	0	0	1.04	0	0	0	1.97	0	81	104

indicating that if this peak corresponds to phosphorylcholine, then the decomposition of phosphorylcholine is faster than that of OPE. Note that we could not obtain a pure standard of phosphorylcholine to confirm its identity.

The other phosphorus products that could appear as peak 6 and 7 could be cyclic glycerophosphates or α- and β-glycerophosphates, or glycerophosphoric acid, as has been suggested previously.[21] Once again these compounds were not available in their pure form, which prohibited their positive identification using NMR. For the unidentified peak 7, its yield increased and then decreased at all temperatures.

The conversion of DOPC was below 0.35 at the mildest conditions examined (*i.e.*, the two shortest reaction times at the two lowest temperatures). Near complete conversion was observed at 225 °C (>60 min) and at all batch holding times at 350 °C. Moreover, a plot of DOPC conversion against the batch holding time displays a sigmoidal behavior (Fig. 3), *i.e.* the conversion increases slowly at shorter batch holding time and then rapidly increases. This behavior is associated with an autocatalytic system and is similar to the behavior observed previously for hydrolysis of ethyl oleate in HTW[8,9] and hydrolysis of triglycerides in sunflower oil.[24]

In the system under consideration, DOPC hydrolysis can likely be catalyzed by oleic acid and by phosphoric acid, as these compounds form during the course of the reaction. To test for catalysis by these acids, we carried out hydrolysis of DOPC at 200 °C and 15 min with different amounts of added oleic acid (equimolar) and phosphoric acid (one and a half times molar concentration of DOPC). Table 2 shows that both the conversion of DOPC and the yield of oleic acid increased in the presence of added acids. Therefore, hydrolysis of DOPC is catalyzed by the oleic acid and phosphoric acid produced during the reaction.

3.2 Reaction pathways

The previous section showed that hydrothermal treatment of DOPC produced a number of products. In this section, we elucidate more fully the reaction pathways for DOPC that lead to these products.

On the basis of the product yields discussed in the previous section, the main primary path for DOPC in HTW is hydrolytic cleavage of a fatty acid moiety linked to the glycerol backbone to form either 1- or 2-acyl LPC (see reactions I and II). This path has been mentioned previously in a number of studies on hydrolysis of phospholipids in liposomal dispersions at low temperature.[16,20,21] 1-Acyl LPC is the major isomer observed in the present work, which is consistent with the results of Grit and coworkers.[18–20] Ester hydrolysis in HTW most commonly follows an Aac2 mechanism wherein protonation of the ester is followed by a nucleophilic attack of water.[25] 1-Acyl LPC is expected to be the major product, since it forms rapidly from 2-acyl LPC *via* acyl migration and is the more stable of the two isomeric forms.[20,26] Hydrolysis of the ester linkages would release oleic acid, which could subsequently catalyze the further hydrolysis of DOPC. Reactions I and II provide a graphical representation of the primary paths for hydrolysis of DOPC.

Note that no path is included for hydrolytic cleavage of the phosphorus-containing moiety. Two possible reactions could

occur here depending on which phosphorus–oxygen bond was cleaved. Cleavage of the choline group would form a 18 : 1 phosphatidic acid (see reaction III), but this product was not observed. The chemical shift of a pure 18 : 1 phosphatidic acid standard did not match any peak in the NMR spectrum shown in Fig. 1. Another possibility is cleavage to form a diglyceride (see reaction IV). We used high-temperature GC but did not detect the diglyceride that would necessarily form in such a path. The absence of the products shown in reactions III and IV indicates that these paths are negligible under the conditions of our investigation. Thus, we exclude these paths from further consideration.

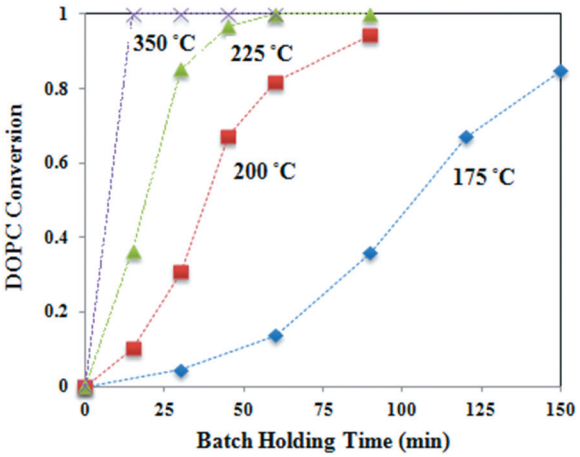

Fig. 3 Temporal variation of DOPC conversion.

Following the formation of the LPC isomers in paths I and II, hydrolysis of the second fatty acid can take place to produce *sn*-glycero-3-phosphorylcholine (GPC), as has been suggested in

Table 2 Conversion of DOPC and yield of oleic acid with and without added acid at 200 °C and 15 min

Acid	DOPC conversion	Oleic acid yield
None	0.10	0.13
Oleic	0.50	0.43
Phosphoric	1.00	1.31

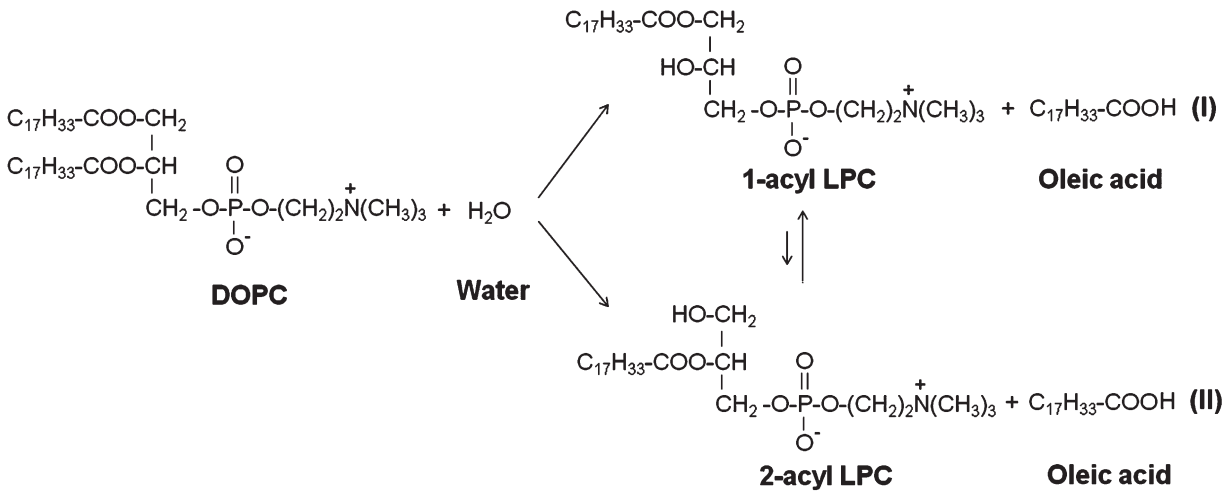

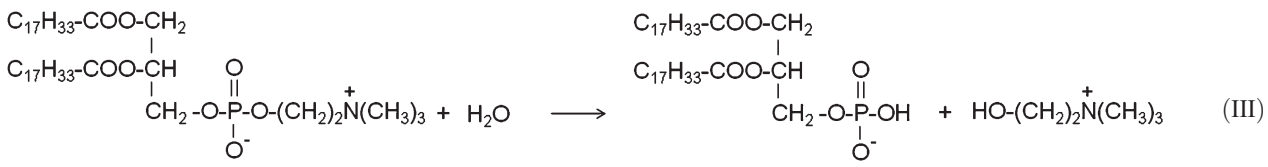

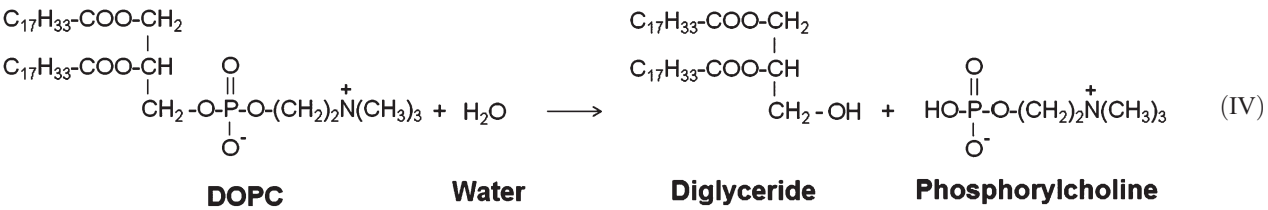

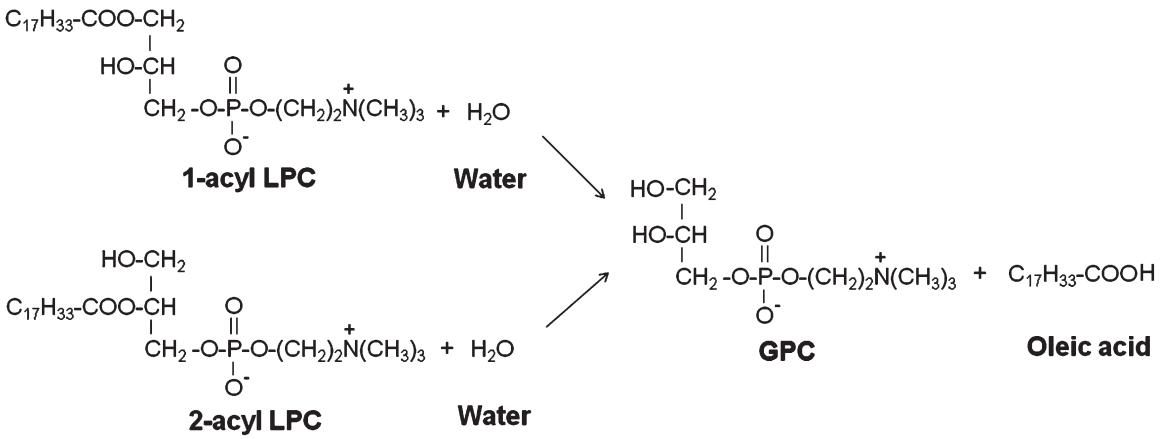

(V)

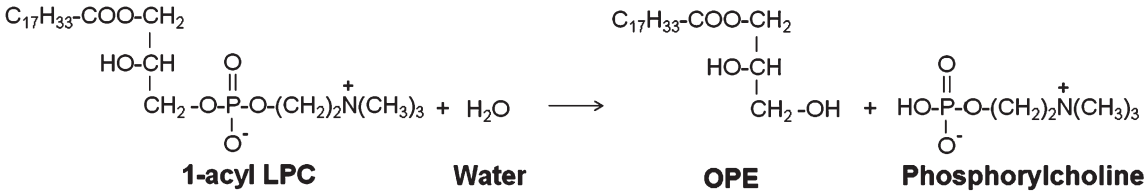

(VI)

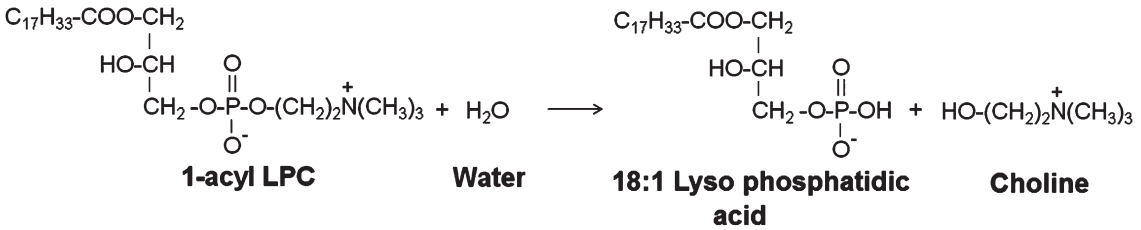

(VII)

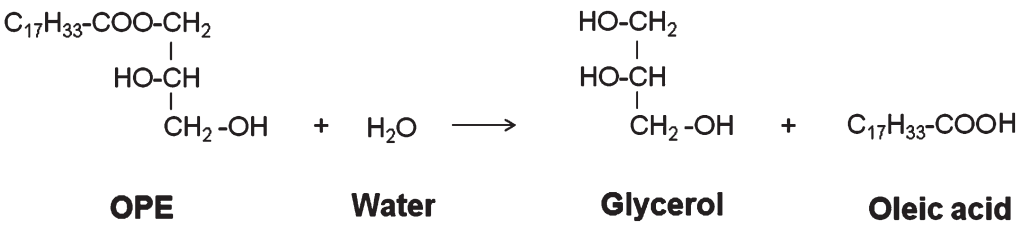

(VIII)

previous work at lower temperatures, see reaction V.[16] Since this step also involves hydrolysis of an ester bond, it could also be catalyzed by the fatty acid produced.

In parallel with the hydrolytic cleavage of the oleate moiety, LPC can also undergo hydrolysis at the phosphate bond in two different ways, similar to reactions III and IV. One possibility is that the 1-acyl LPC, being the major isomer, would form 9-octadecenoic-2,3-dihydroxypropyl ester (OPE) (reaction VI), consistent with our observation of this compound as one of the reaction products. Phosphorylcholine would also be released as a co-product of this reaction. Alternatively, 1-acyl LPC could liberate choline and form 18 : 1 lyso-phosphatidic acid (see reaction VII). However, none of the peaks in the NMR spectra corresponded to a pure standard of 18 : 1 lyso-phosphatidic acid. Therefore, reaction VII seems unlikely under these conditions and has been excluded from further consideration.

OPE, once formed in reaction VI, can hydrolyze further to liberate glycerol and oleic acid as shown in reaction (VIII). Once again, OPE hydrolysis can be catalyzed by oleic acid and phosphoric acid.

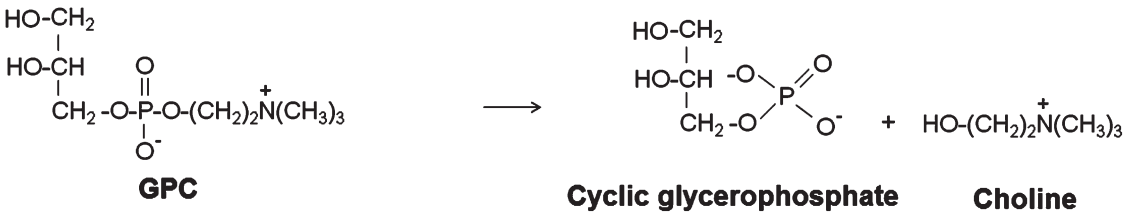

(IX)

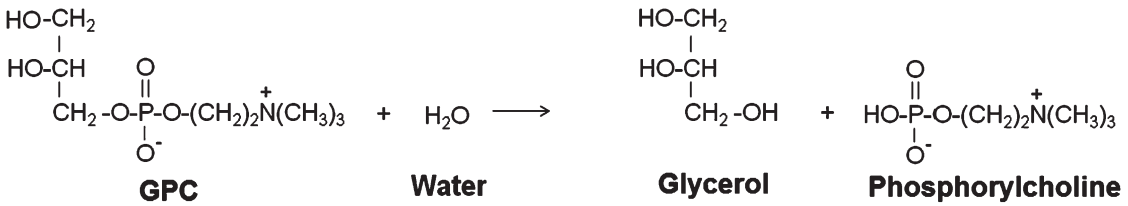

(X)

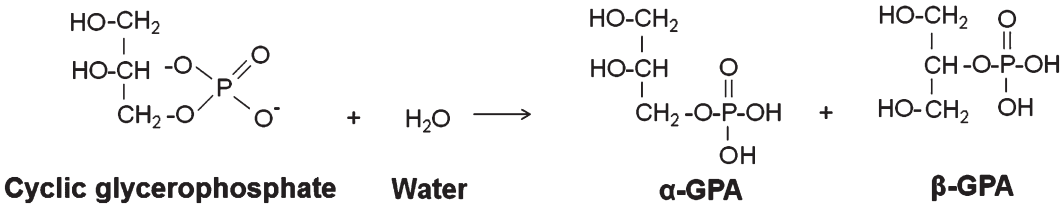

(XI)

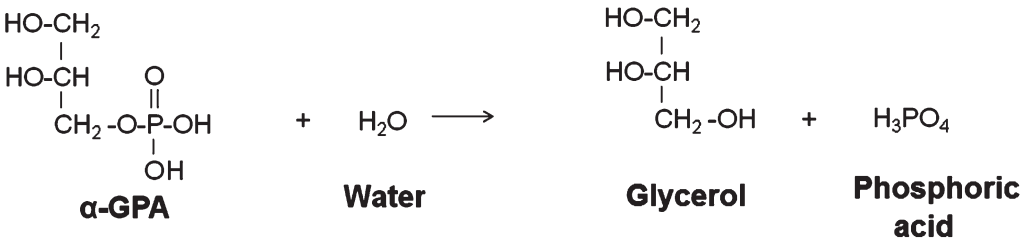

(XII)

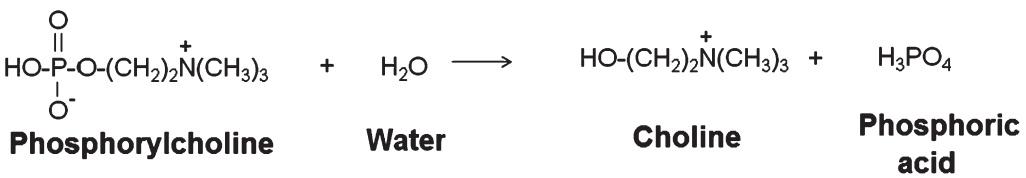

(XIII)

GPC, formed in path V, could react at either of the two P–O bonds, giving rise to two parallel reactions.[17,21] Protonation of the oxygen between the phosphorus atom and the choline moiety can occur *via* a cyclic *ortho* triester to form cyclic glycerophosphate and choline (reaction IX). In a parallel reaction, protonation of oxygen between the glycerol carbon and phosphorus can occur to release glycerol and phosphorylcholine (reaction X). Koning and McMullan mention that under acidic conditions, reaction IX is favored over reaction X, *i.e.* more cyclic glycerophosphate is formed than phosphorylcholine.[21]

Cyclic glycerophosphate can be converted to an equilibrium mixture of α- and β-glycerophosphate or glycerophosphoric acid (GPA), depending on the pH, as shown in reaction XI. Usually the α-GPA is the major product.[17,22]

Glycerophosphate can further hydrolyze to release phosphoric acid and glycerol, both of which were observed as products in this investigation (reaction XII).

Lastly, phosphoric acid could also be formed *via* the hydrolysis of phosphorylcholine, see reaction XIII. This reaction also liberates a choline molecule.

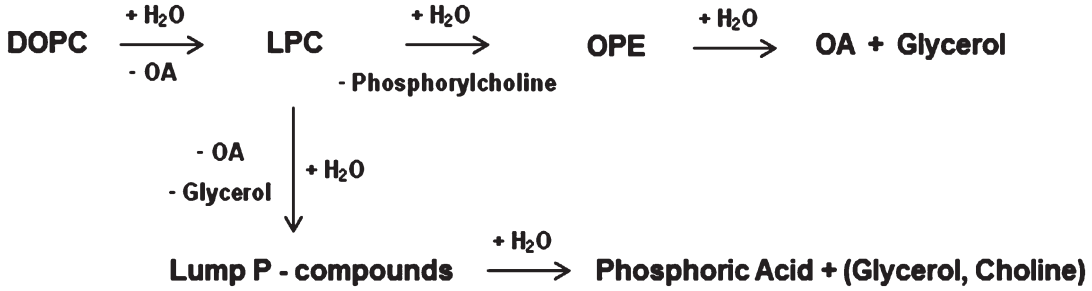

Fig. 4 Streamlined reaction network for DOPC in HTW.

This section has summarized the different reaction pathways likely to be operative for the reaction of DOPC in HTW. We offer these pathways on the basis of the literature and the experimental results reported in the previous section. Other phospholipids could potentially undergo similar chemistry in HTW.

3.3 Kinetics model

In this section, we use the reaction pathways just discussed as the basis for a quantitative kinetics model. Fig. 4, a simplified reaction network for DOPC in HTW, accounts for the reactions outlined in the previous section. We have streamlined the reaction network by lumping the 1- and 2-acyl LPC isomers together and denoting them as LPC. Additionally, we lumped together all of the phosphorus-containing products of LPC since we did not quantify all of these products and some of their identities are tentative.

This streamlined reaction network contains five different hydrolytic pathways. On the basis of our previous work with ethyl oleate hydrolysis,[8,9] wherein, hydrolysis of ester linkages was found to be catalyzed by acid, we allow each of the hydrolytic paths to be catalyzed by both oleic acid and phosphoric acid. Thus, this network can be represented by a set of 15 individual reactions as shown on the following pages. The first group of five reactions in this set is uncatalyzed, the next set of five reactions is catalyzed by oleic acid, and the last set of five reactions is catalyzed by phosphoric acid.

We assume that all reactions are irreversible (since water was present in large excess) and first-order in each reactant. We do not include the concentration of water in the rate equations since it did not change appreciably during the reaction. We obtain numerical values for the rate constants for the individual reaction paths by fitting the experimental product concentrations to the model equations (eqn (1) –(6)), which apply to this reaction network and the constant-volume batch reactors used in the experiments.

$$\frac{dC_1}{dt} = -k_1C_1 - k_6C_1C_4 - k_{11}C_1C_6 \quad (1)$$

$$\frac{dC_2}{dt} = k_1C_1 - k_2C_2 - k_3C_2 + k_6C_1C_4 - k_7C_2C_4 - k_9C_2C_4 + k_{11}C_1C_6 - k_{12}C_2C_6 - k_{14}C_2C_6 \quad (2)$$

$$\frac{dC_3}{dt} = k_3C_2 - k_4C_3 - k_8C_3C_4 + k_9C_2C_4 - k_{13}C_3C_6 + k_{14}C_2C_6 \quad (3)$$

$$\frac{dC_4}{dt} = k_1C_1 + k_2C_2 + k_4C_3 + k_6C_1C_4 + k_7C_2C_4 + k_8C_3C_4 + k_{11}C_1C_6 + k_{12}C_2C_6 + k_{13}C_3C_6 \quad (4)$$

$$\frac{dC_5}{dt} = k_2C_2 + k_3C_2 - k_5C_5 + k_7C_2C_4 + k_9C_2C_4 - k_{10}C_5C_4 + k_{12}C_2C_6 + k_{14}C_2C_6 - k_{15}C_5C_6 \quad (5)$$

$$\frac{dC_6}{dt} = k_5C_5 + k_{10}C_5C_4 + k_{15}C_5C_6 \quad (6)$$

C is the concentration and the subscripts 1–6 represent DOPC, LPC, OPE, oleic acid, lumped P-containing compounds, and phosphoric acid, respectively. We used *fmincon* in MATLAB to solve simultaneously the set of ordinary differential equations above and perform parameter estimation to obtain the values of the rate constants at a given temperature.[27] The objective function for minimization was the summation of squared relative error (SSRE) between the calculated and experimental product concentrations at a given reaction temperature. This quantity was calculated using eqn (7), where j is the number of discrete reaction times at a particular temperature and i is the number of components.

$$\mathrm{SSRE} = \sum_j \sum_{i=1}^{6} \left[\frac{C_{j,i,\mathrm{model}} - C_{j,i,\mathrm{exp}}}{(C_{j,i,\mathrm{model}} + C_{j,i,\mathrm{exp}})/2} \right]^2 \quad (7)$$

The rate constants at each temperature were then fit to the linearized form of the Arrhenius equation to get A_i and E_{a_i} along with the associated standard errors for each rate constant.

Table 3 gives the Arrhenius parameters for the DOPC reaction network and the rates for the different reaction steps at 200 °C and 60 min. Reactions 1, 6, and 11 all represent the same pathway (hydrolysis of DOPC), but steps 6 and 11 are catalyzed. The rate of the uncatalyzed path is nearly two and a half times less than that for the oleic acid catalyzed path and almost equal to that for the phosphoric acid catalyzed path. Reactions 2, 7, and 12 also represent the same pathway (hydrolysis of LPC), with steps 7 and 12 being catalyzed. For this path, the uncatalyzed step is orders of magnitude slower than the catalyzed paths. The same is found to be true when comparing the rates of reactions 4, 8, and 13, which

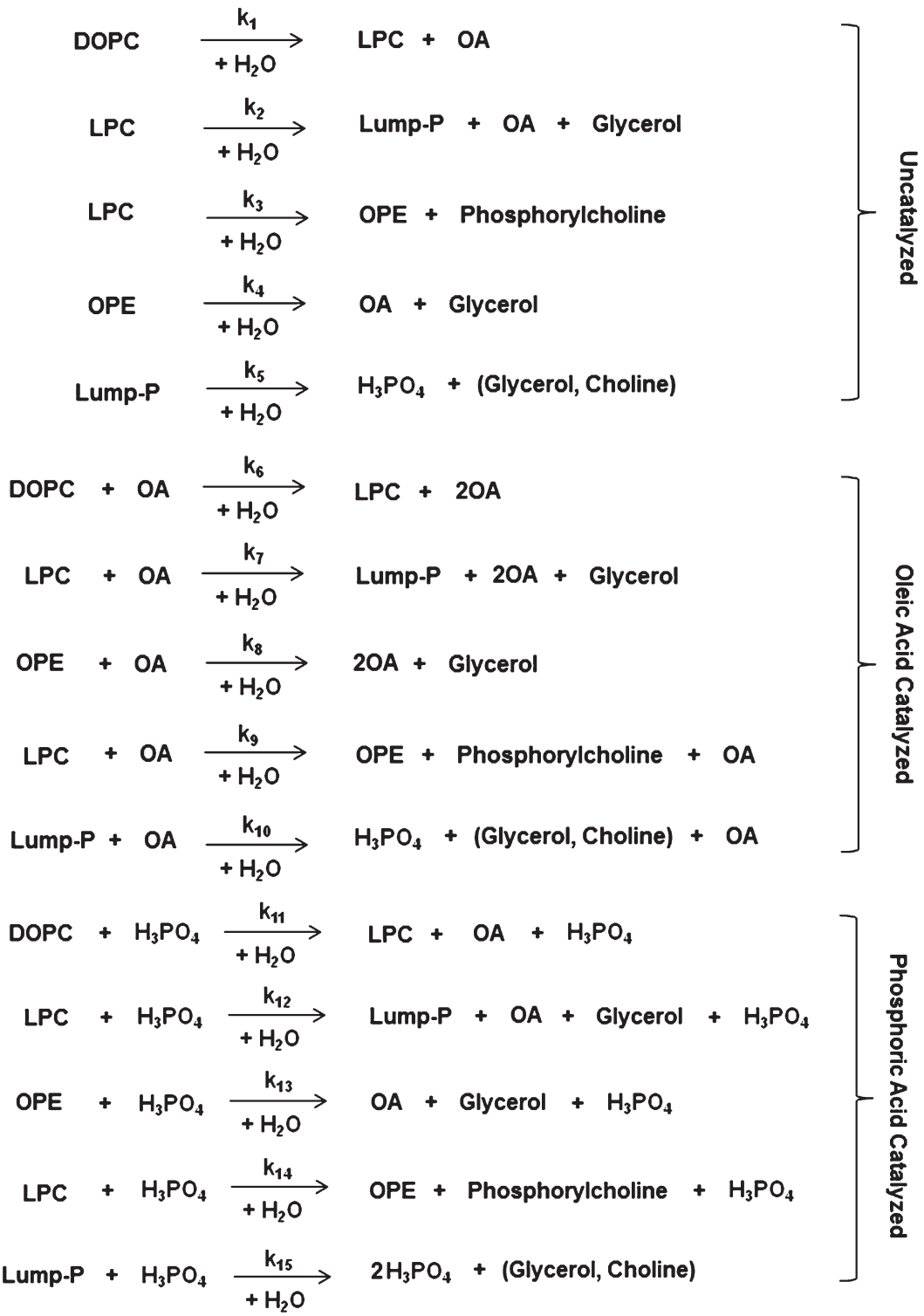

describe OPE hydrolysis. Since the rates of uncatalyzed paths 2 and 4 are negligible at conditions of Table 3 and more generally at all times at 200 °C, we removed these paths from the model and fit the data again using just thirteen rate constants. Removing these two parameters did not change the other rate constants.

Fig. 5 shows the parity plot for the experimental and calculated concentrations of the different chemical species. The dotted diagonal line represents a perfect fit of the model to the experimental data, and the dotted lines above and below represent ±20% error. Fig. 5a shows that the model generally fits the experimental data for the major products to within ±20% and also predicts the concentrations of the major products at 350 °C well. Moreover, the data are scattered on both sides of the diagonal, indicating the absence of systematic error. Fig. 5b shows that there is more scatter for the minor products, but even here the model often fits the data to within the experimental uncertainty.

3.4 Implications for hydrothermal processing of algae

The results from this study of DOPC reactions in HTW have several implications for hydrothermal liquefaction of algae. The production of fatty acid from phospholipids being autocatalyzed has implications for process design and optimization for hydrothermal biofuel production process. Autocatalytic reactions exhibit a maximum rate at some intermediate conversion. Designing to operate at this maximum rate would minimize the total reactor volume required.

In an ideal process, all of the phosphorus atoms would reside in compounds that partition into the aqueous, rather than organic, phase after hydrothermal processing. This outcome would provide a phosphorus-free fuel product and a phosphorus-rich aqueous stream that can be used to grow more algal biomass. Many of the phosphorus-containing compounds reported here (α-, β-GPA, phosphorylcholine) would likely distribute themselves into the organic phase, whereas phosphoric acid would go into the aqueous phase. Thus, phosphorus recycling after hydrothermal processing of algae would be facilitated by processing at conditions that produce phosphoric acid as the sole phosphorus-containing product. This study provides a reaction network and kinetics of different pathways that can be useful for identifying these conditions. For example, the model predicts that at an isothermal temperature of 300 °C a reaction time of at least 8 min is required to convert 99% of the phosphorous in DOPC into phosphoric acid.

Table 3 Arrhenius parameters for DOPC reaction network

Index no.	log A	E_a (kJ mol^{-1})	Units of k_i	Rate 200 °C, 60 min (mol L^{-1} min^{-1})
1	6.4 ± 0.5	77 ± 5	min^{-1}	1.84E-4
2	7.5 ± 0.7	119 ± 6	min^{-1}	2.83E-8
3	5.9 ± 2.9	72 ± 27	min^{-1}	1.24E-4
4	13.7 ± 4.4	192 ± 40	min^{-1}	2.64E-10
5	11.9 ± 3.1	122 ± 28	min^{-1}	5.45E-4
6	4.1 ± 1.7	42 ± 16	min^{-1} mol^{-1} L	4.75E-4
7	7.8 ± 0.4	71 ± 4	min^{-1} mol^{-1} L	8.33E-4
8	18.3 ± 4.6	182 ± 42	min^{-1} mol^{-1} L	2.31E-5
9	10.8 ± 4.8	111 ± 43	min^{-1} mol^{-1} L	3.45E-5
10	6.2 ± 1.1	64 ± 10	min^{-1} mol^{-1} L	1.92E-4
11	4.7 ± 1.5	47 ± 14	min^{-1} mol^{-1} L	1.15E-4
12	16.5 ± 3.9	151 ± 36	min^{-1} mol^{-1} L	1.10E-4
13	14.9 ± 7.2	162 ± 65	min^{-1} mol^{-1} L	1.37E-7
14	3.5 ± 0.4	37 ± 3	min^{-1} mol^{-1} L	4.75E-5
15	7.6 ± 0.3	72 ± 3	min^{-1} mol^{-1} L	1.29E-4

Conclusion

Under the conditions studied, DOPC hydrolyzed to form oleic acid, several phosphorus-containing compounds, glycerol, and choline. We also detected an ester of oleic acid and glycerol (OPE), which had not been documented previously. The conversion for DOPC showed a sigmoidal trend with increasing batch holding time, indicating catalysis by oleic and phosphoric acid, which was also confirmed experimentally.

The primary paths from DOPC form 1-acyl LPC and 2-acyl LPC, which subsequently hydrolyze *via* parallel reactions to form either OPE or α-GPA + β-GPA + phosphorylcholine, *via* GPC. Hydrolysis of both DOPC and LPC releases oleic acid. Phosphoric acid was the sole phosphorus-containing end product. A phenomenological kinetics model based on these pathways accurately describes the trends in the data and typically estimates the species concentrations to within their experimental errors.

The results from this study of DOPC in HTW have implications to algae processing. For instance, the existence of autocatalysis influences process design decisions, and the reaction network can be used to identify processing conditions that facilitate recycling phosphorus in the aqueous phase for additional biomass growth.

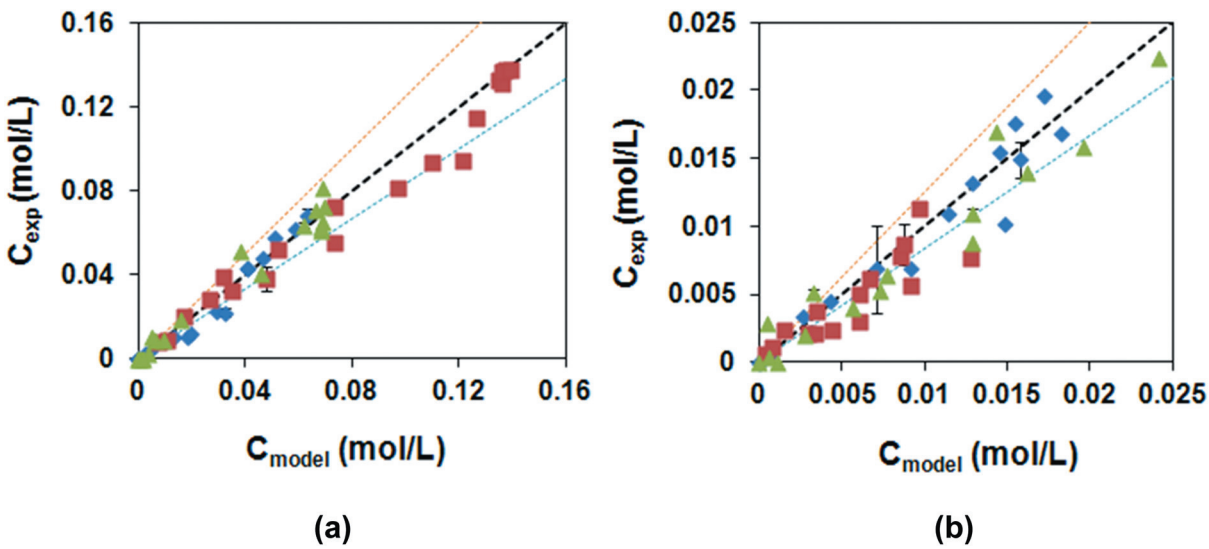

Fig. 5 Comparison of experimental and calculated concentrations at 175 °C, 200 °C, 225 °C, and 350 °C for (a) ◆ DOPC ■ oleic acid ▲ phosphoric acid and (b) ◆ LPC ■ OPE ▲ lumped P-compounds.

Acknowledgements

We gratefully acknowledge Mr Eugenio Alvardo and Mr Chris Kojiro for training in NMR and assistance in quantifying phosphorus-containing compounds. We also acknowledge financial support from the National Science Foundation (EFRI 0937992).

References

1 J. A. V. Costa and M. G. de Morais, The role of biochemical engineering in the production of biofuels from microalgae, *Bioresour. Technol.*, 2011, **102**, 2–9.
2 T. M. Mata, A. A. Martins and N. S. Caetano, Microalgae for biodiesel production and other applications: A review, *Renewable Sustainable Energy Rev.*, 2010, **14**, 217–232.
3 T. M. Brown, P. Duan and P. E. Savage, Hydrothermal liquefaction and gasification of *Nannochloropsis* sp., *Energy Fuels*, 2010, **24**(6), 3639–3646.
4 R. B. Levine, T. Pinnarat and P. E. Savage, Biodiesel production from wet algal biomass through in situ lipid hydrolysis and supercritical transesterification, *Energy Fuels*, 2010, **24**, 5235–5243.
5 S. M. Heilmann, H. T. Davis, L. R. Jader, P. A. Lefebvre, M. J. Sadowsky, F. J. Schendel, M. G. von Keitz and K. J. Valentas, Hydrothermal carbonization of microalgae, *Biomass Bioenergy*, 2010, **34**(6), 875–882.
6 Q. Guan and P. E. Savage, Gasification of *Nannochloropsis* sp. in supercritical water, *J. Supercrit. Fluids*, 2012, **61**, 139–145.
7 P. E. Savage, Organic chemical reactions in supercritical water, *Chem. Rev.*, 1999, **99**, 603–621.
8 S. Changi, T. Pinnarat and P. E. Savage, Modeling hydrolysis and esterification kinetics for biofuel processes, *Ind. Eng. Chem. Res.*, 2011, **50**(6), 3206–3211.
9 S. Changi, T. Pinnarat and P. E. Savage, Mechanistic modeling of hydrolysis and esterification kinetics for biofuel processes, *Ind. Eng. Chem. Res.*, 2011, **50**(22), 12471–12478.
10 S. Changi, T. M. Brown and P. E. Savage, Reaction kinetics and pathways for phytol in high- temperature water, *Chem. Eng. J.*, 2012, **189**, 336–345.
11 S. Changi, M. Zhu and P. E. Savage, Hydrothermal reaction kinetics and pathways of phenylalanine alone and in binary mixtures, *ChemSusChem*, 2012, DOI: 10.1002/cssc.201200146.
12 E. W. Becker, *Microalgae: Biotechnology and Microbiology*, Cambridge University Press, Cambridge, 1994.
13 D. S. Bailey and D. H. Northcote, Phospholipid composition of the plasma membrane of the green alga, *Hydrodictyon africanum*, *Biochem. J.*, 1976, **156**, 295–300.
14 K. Fahl and G. Kattner, Lipid content and fatty acid composition of algal communities in sea-ice and water from the Weddell Sea (Antarctica), *Polar Biol.*, 1993, **13**, 405–409.
15 N. J. Zuidam and D. J. A. Crommelin, Chemical hydrolysis of phospholipids, *J. Pharm. Sci.*, 1995, **84**(9), 1113–1119.
16 C. R. Kensil and E. A. Dennis, Alkaline hydrolysis of phospholipids in model membranes and the dependence on their state of aggregation, *Biochemistry*, 1981, **20**, 6079–6085.
17 D. J. Hanahan, *Lipide Chemistry*, John Wiley & Sons, Inc., New York, 1960.
18 M. Grit, J. H. de Smidt, A. Struijke and D. J. A. Crommelin, Hydrolysis of phosphatidylcholine in aqueous liposome dispersions, *Int. J. Pharm.*, 1989, **50**, 1–6.
19 M. Grit and D. J. A. Crommelin, The effect of aging on the physical stability of liposome dispersions, *Chem. Phys. Lipids*, 1992, **62**, 113–122.
20 M. Grit and D. J. A. Crommelin, Chemical stability of liposomes: implications for their physical stability, *Chem. Phys. Lipids*, 1993, **64**, 3–18.
21 A. J. De Koning and K. B. McMullan, Hydrolysis of phospholipids with hydrochloric acid, *Biochim. Biophys. Acta, Lipids Lipid Metab.*, 1965, **106**, 519–526.
22 B. Maruo and A. A. Benson, Cyclic glycerophosphate formation from the glycerolphosphatides, *J. Biol. Chem.*, 1959, **234**(2), 254–256.
23 http://www.umich.edu/~chemnmr/docs.html, Date last accessed 12th April, 2012.
24 R. Alenezi, G. A. Leeke, R. C. D. Santos and A. R. Khan, Hydrolysis kinetics of sunflower oil under subcritical water conditions, *Chem. Eng. Res. Des.*, 2009, **87**, 867–873.
25 J. N. E. Day and C. K. Ingold, Mechanism and kinetics of carboxylic ester hydrolysis and carboxyl esterification, *Trans. Faraday Soc.*, 1941, **37**, 686–705.
26 A. Plückthun and E. A. Dennis, Acyl and phosphoryl migration in lysophospholipids: importance in phospholipid synthesis and phospholipase specificity, *Biochemistry*, 1982, **21**, 1743–1750.
27 http://www.mathworks.com/help/toolbox/optim/ug/fmincon.html. Date last accessed, 3rd September 2011.